Journal of Physics:
Conference Series

PURPOSE-LED PUBLISHING™

PAPER • **OPEN ACCESS**

Operational Modal Analysis and Mode Tracking of the WiValdi OPUS-2 Wind Turbine

To cite this article: Giulia Jelicic *et al* 2026 *J. Phys.: Conf. Ser.* **3224** 062067

View the article online for updates and enhancements.

You may also like

- Modal Analysis of a Quad-Rotor Wind Turbine
Etana Ferede and Farhan Gandhi
- Research sized wind turbine blade modal tests: comparison of the impact excitation with shaker excitation
M. M. Luczak, B. Peeters, S. Manzato et al.
- Aeroelastic Stability Analysis of a Quad-Rotor Wind Turbine
Etana Ferede, Alexander Stillman and Farhan Gandhi

Enabling Electrochemistry Inside and Outside the Lab

PalmSens

Discover our diverse range of Potentiostats engineered to support your research wherever it takes you

- Intuitive software for Windows and Android
- Proven in over 4000 scientific publications
- Single-channel and multi-channel
- Benchtop, portable and wearable

Discover More



This content was downloaded from IP address 129.247.247.240 on 05/11/2026 at 15:34

Journal of Physics: Conference Series **3224** (2026) 062067 doi:10.1088/1742-6596/3224/6/062067

Operational Modal Analysis and Mode Tracking of the WiValdi OPUS-2 Wind Turbine

Giulia Jelicic[1], **Kevin Gnebner**[1] **and Yves Govers**[1]

[1]Institute of Aeroelasticity, German Aerospace Center (DLR), Göttingen, Germany

E-mail: g.jelicic@dlr.de

Abstract. The present paper investigates the experimental determination of the parameter-dependent eigenfrequency, damping ratio and mode shapes of the parked WiValdi OPUS-2 wind turbine using operational modal analysis. A data-driven dynamic model is constructed as a function of environmental and operational parameters. Accelerometers are placed on both the rotor and the tower to allow a better separation of eigenmodes. Data is collected over one year to cover a wide parameter space. More than twenty eigenmodes can be identified and tracked in the lower frequency range. It is possible to separate closely-spaced modes such as the tower fore-aft and side-side bending. Detailed results are presented for the first two tower bending modes, the two first rotor collective modes and the first rotor asymmetric mode. The damping ratio is shown to have a direct dependency on wind speed and yaw misalignment.

Keywords: *wind turbine testing; operational modal analysis; damping estimation*

1. Introduction

A massive expansion of renewable energy sources is necessary for a reliable, affordable, and environmentally friendly energy, which comes with increasing efficiency and social acceptance. The German Aerospace Center (DLR), collaborating with the Research Alliance Wind Energy, is expanding the WiValdi research facility [1]. The scientific goals of the wind park are more efficient, quieter, and more cost-effective wind turbines. To this end, the facility features meteorological masts and extensive instrumentation on its wind turbines.

The modal parameters of wind turbines are dependent on operating conditions and aeroelastic phenomena. A better understanding of their dynamics is obtained through data-driven approaches [2][3]. In the current state of the art, modal parameter uncertainty and mode tracking are performed mostly on instrumented towers [4][5]. Existing investigations on the WiValdi facility include experimental and methodological modal analysis results from rotor blades before installation and from the meteorological mast [6][7][8]. There are still gaps in the full-scale analysis with instrumented rotor and in how operational and environmental conditions affect the modal parameters and their uncertainty.

This study focuses on the estimation, tracking and uncertainty quantification of the modal parameters of the parked WiValdi OPUS-2 wind turbine. This is accomplished by operational modal analysis of measured accelerations on both rotor and tower. We show that it is possible to identify and track more than twenty eigenmodes across a range of wind speeds, yaw angles and wind directions. The resulting data-driven modal model supports ongoing research activities (validation of finite element models, controller synthesis and structural health monitoring).


Content from this work may be used under the terms of the Creative Commons Attribution 4.0 licence. Any further distribution of this work must maintain attribution to the author(s) and the title of the work, journal citation and DOI.
Published under licence by IOP Publishing Ltd

2. Experimental setup

The WiValdi wind park is located on the German North Sea coast in the vicinity of the mouth of the Elbe. It features two main Enercon E115 EP3 4.26 MW wind turbines. The OPUS-2 wind turbine has a rotor diameter of 115 m, a hub height of 92 m. Three meteorological masts acquire various atmospheric data that is available together with structural data. In the present analysis we are interested in the structural dynamic properties of the parked wind turbine (rotation is prevented by bolts inserted into the rotor). By measuring the accelerations from both the rotor and tower, a better separation of closely-spaced eigenmodes is possible.

The measurement setup consists of 68 accelerometers as illustrated in figure 1:

- 17 tower accelerometers at 8 different heights starting from 19 m. 9 are along the main wind direction and 8 in the perpendicular direction. When the rotor is facing the wind, the former correspond to the fore-aft motion, the latter to the side-side motion.
- 17 accelerometers on each rotor blade up to half the blade length. 7 are positioned at the leading edge in the edge-wise direction. 10 are oriented along the flap-wise direction (7 at the leading edge and 3 on the trailing edge). When the wind turbine is parked, edge-wise corresponds to fore-aft and flap-wise to side-side.

The rotor and tower accelerometers are sampled at 200 Hz. In the present analysis, only a subset of all available accelerometers on the OPUS-2 wind turbine has been selected. Due to lightning protection the sensors may not be placed beyond half the blade span. Wind turbine operational/control parameters and various meteorological data are acquired simultaneously but with different sample rates. Relevant for this analysis are wind data, rotor position, blade pitch and nacelle yaw.

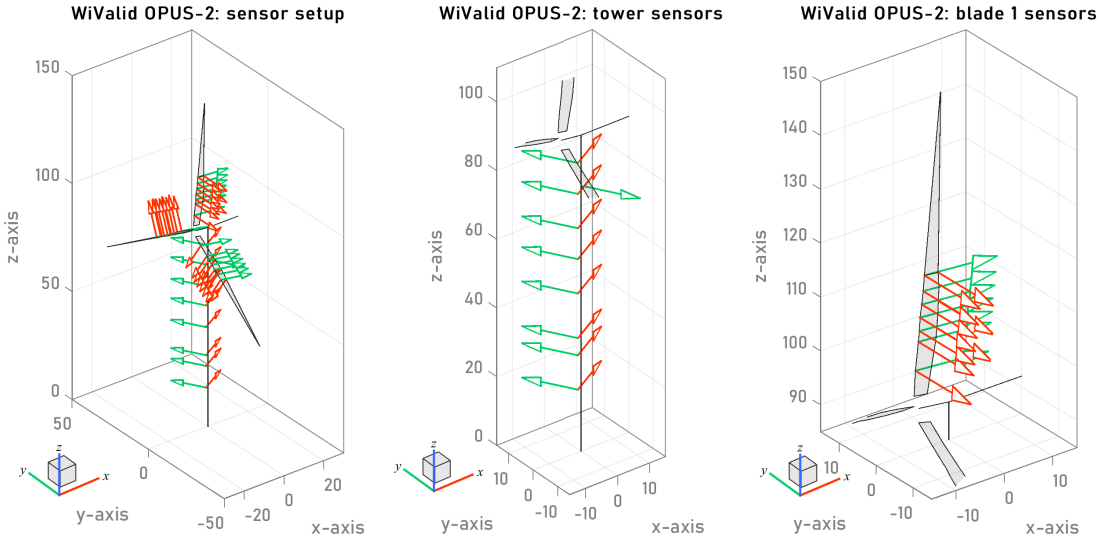


Figure 1. OPUS-2 wind turbine sensor setup. The tower, nacelle and hub are represented by a line; the rotor blades are idealized by a polygon and pitched in the parked position. Each arrow represents the actual position and orientation of an accelerometer. Left subfigure: overview. Center subfigure: tower accelerometers (green: main wind direction, red: perpendicular to the main wind direction). In this figure the green arrows are approximately in the side-side direction. Right subfigure: accelerometers on a rotor blade (green: edge-wise direction, red: flap-wise direction).

3. Data selection

Modal analysis is performed on the parked wind turbine. The wind turbine is considered parked when its controller reports a "locked" state (i.e. the rotor is mechanically fixed). The selection is not performed based on the rotor speed (which may be idling). Data records with a duration of 10 minutes where the wind turbine is locked are retrieved from a period of one year. The records are further filtered to eliminate impulsive events (e.g. no blade pitch or nacelle yawing within 10 minutes, sensor drop-outs, maintenance etc..) and to cover a wide parameter space (e.g. with respect to wind speed, turbulence, rotor position and yaw angle). The final selection of 420 data sets spans a period of approximately 37 weeks from November 2024 to September 2025. Figure 2 displays the wind conditions and operational parameters of the data sets, while figure 3 shows the histograms of some of the wind conditions and operational parameters. Wind speeds range from 0.5 m/s up to 12.1 m/s. More than ninety percent of the data sets have a turbulence intensity between 6% and 35%, effectively covering the entire wind speed range. The difference between wind direction and nacelle yaw is within 50 degrees. The dominant wind direction is at around 240 deg (wind coming from south-west). The rotor azimuth modulo 120 is concentrated at 30, 60 and 90 deg (one blade points at 1, 2 and 3 o'clock).

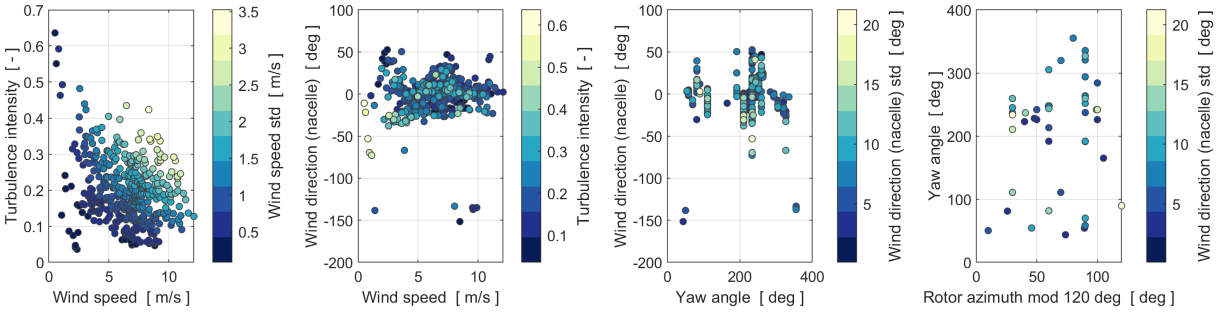


Figure 2. Wind conditions and operational parameters for the locked wind turbine (420 data sets). The rotor position or blade pitch angles do not change within one data set. The nacelle does not actively align with the wind. In the axes' labels: "*std*" is the standard deviation.

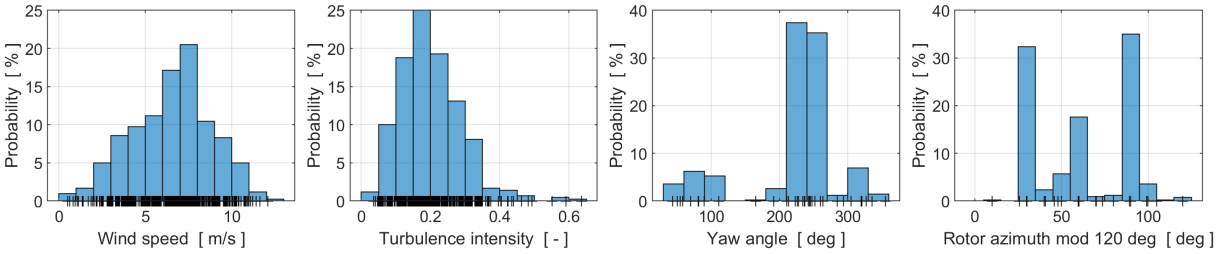


Figure 3. Histograms of wind conditions and operational parameters. See text for discussion.

4. Methodology

System identification is performed in time-domain within the operational modal analysis framework using measured accelerations [9]. Time data is decimated to reduce the frequency bandwidth for system identification and to remove high-frequency signal spikes. The identified model structure is a stochastic state-space model with unknown noise input and with process and measurement noise contributions. The modal parameters are identified by the covariance-based

stochastic subspace identification (SSI) algorithm with variance estimation [10]. A review of SSI methods applied to mechanical engineering can be found in [11]. The modal parameters variance is estimated in order to better separate the physical system poles from mathematical fitting artifacts and for weighting down badly-estimated eigenmodes. Estimating the modal parameter variance for several model orders has a considerable impact on calculation time. The validation of the identified modal modal for each record is performed by comparing the measured and the reconstructed power spectral density of the output signals. In a last step, the modal parameters identified from each record are tracked and sorted into mode clusters. For mode tracking: the mode shape tower components are projected onto the fore-aft/side-side frame; the mode shape components on the rotor are projected in a fixed frame via Coleman transformation [12].

5. Results

5.1. Spectral estimation

Output data for OMA methods are tacitly assumed to be normally-distributed. The skewness and excess kurtosis estimates of all data records have been inspected to identify sensors with abnormal conditions, asymmetry in the response and presence of outliers. Strong deviations from this assumption affect negatively system identification and render spectral estimation results difficult to interpret. Figure 4 displays the autopower spectral density (APSD) of three sensors from all records as a function of wind speed. The APSD is estimated using the multi-taper method to obtain a higher frequency resolution compared to Welch's modified periodogram [13]. The APSD reveals that the resonances (eigenfrequencies) do not vary much with wind speed. This nonparametric method does not resolve closely-spaced modes, such as the tower bending at $f = 0.5$. The excitation level is lower at low wind speeds, therefore some modes of vibration are not well excited and identified with less confidence. On the other hand, higher wind speeds tend to correlate with less stationary conditions.

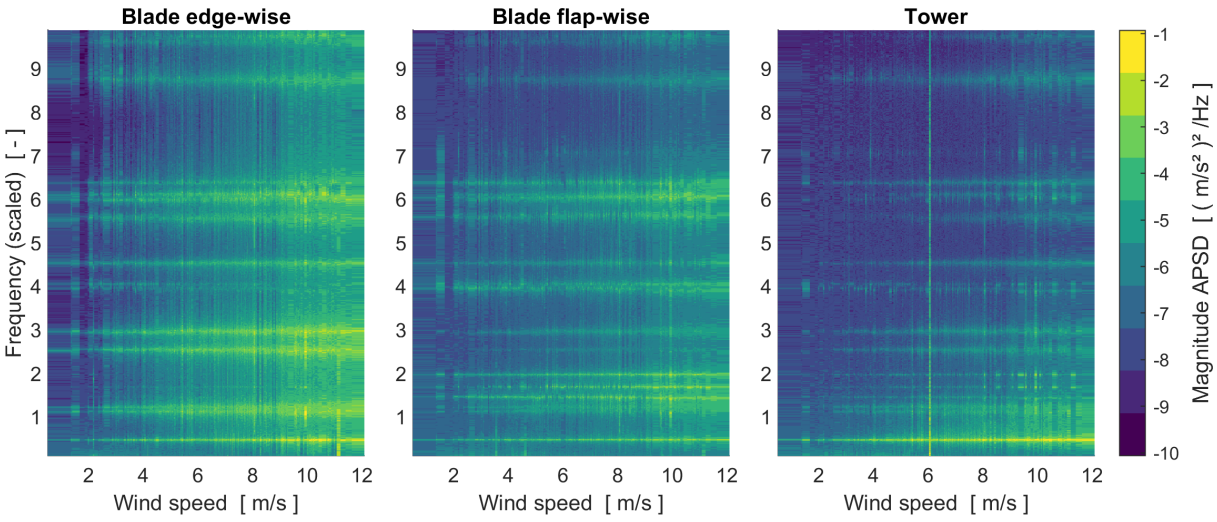


Figure 4. Autopower spectral density (APSD) as a function of wind speed. (signals from one accelerometer at the highest tower position and two accelerometers at the maximal span-wise distance of one blade). Each image consists of stacked and sorted APSD estimates (not a spectrogram). The colormap (magnitude) limits are the same for all subplots. The APSD is estimated using the multi-taper method. The vertical line in the rightmost subfigure is a faulty sensor.

5.2. System identification

For each record the modal parameters are identified for several model orders and displayed in a stabilization diagram (see figure 5). The model order of the system is not known a priori and must be estimated since it determines the maximal number of eigenmodes within a given frequency band. The minimal model order is estimated by fitting the noise floor using the method described in [14]. Based on a reconstruction accuracy of at least 90%, a minimal model order 30 is selected. The maximal model order 70 is chosen based on a bias-variance trade-off. The hierarchical clustering technique described in reference [15] implements the selection of the model order that results in the lowest validation error. Spurious poles that present large variations in eigenfrequency or damping ratio between two consecutive model orders can be removed using the technique in [16]. The mode shapes of the eigenmodes from table 1 are displayed in figure 8. More details are provided in the next paragraphs.

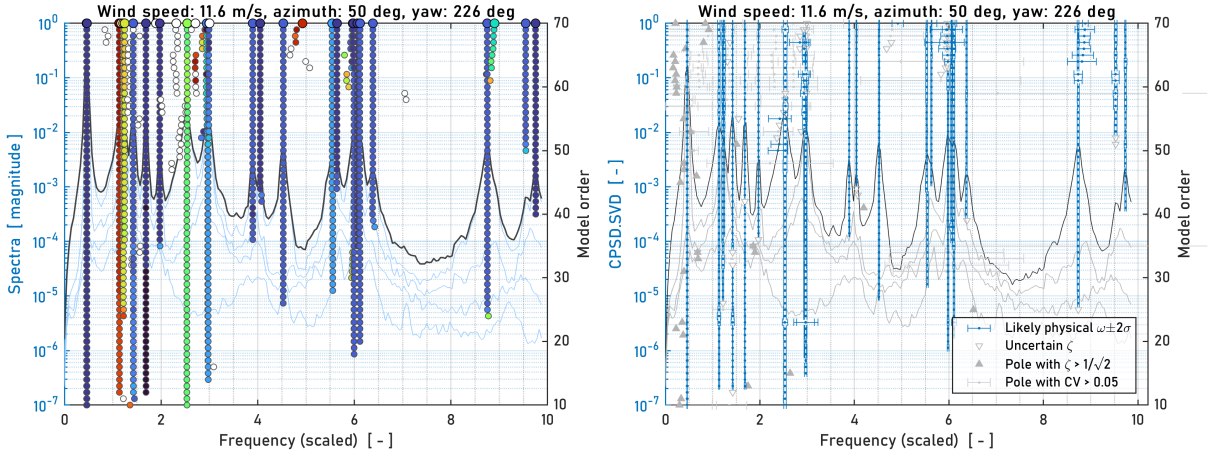


Figure 5. Stabilization diagram of one data set. The eigenfrequency and damping ratio are scaled due to confidentiality. Left subfigure: the marker color represents the damping ratio (blue: low, red: high, white: out-of-bounds). The larger markers represent the modal model. Right subfigure: the error bars represent the eigenfrequency variance estimates. Poles that have high variance, high damping or uncertain damping estimates are grayed out. See text for discussion.

5.3. Mode tracking

An automated mode tracking procedure is employed to gather, filter and name the eigenmodes. The goal is to obtain large distinct mode families of few physical eigenmodes and many small unrelated mode families of spurious eigenmodes. This operation is similar to the labelling performed by hierarchical clustering, for instance as shown in reference [15]. For the data sets at hand, tracking over a physical parameter affecting the system's dynamics (e.g. wind speed, turbulence, rotor azimuth or nacelle yaw) has been found to be more effective. We use therefore the mode tracking technique detailed in [13]. The algorithm assigns each eigenmode to a mode cluster where other similar eigenmodes are found. The similarity is evaluated by defining a "distance" between two eigenmodes. In this analysis we employ the MAC-weighted hyperbolic distance from [17] and the MACXP criterion proposed in [18]. The MAC value alone is not sufficient for tracking, as there are several closely-spaced modes (e.g. referring to figures 5 and 7, the first fore-aft and side-side tower modes at $f = 0.5$ and the first rotor modes at $f = 1.1$). The selected distance metrics take into account both the location of the poles on the complex plane and their mode shapes.

The global results of mode tracking results are illustrated in figure 6 (eigenfrequency over wind speed and damping ratio over eigenfrequency). In figure 6 it is possible to observe several closely-spaced modes, for instance around $f = 0.5$ (first tower bending modes) and $f = 1.1$ (first rotor bending modes). The scatter of the identified damping ratio is due to noise overlaid with an increasing trend due to increasing wind speed. The eigenfrequency variation due to wind speed is found to be much weaker compared to the damping ratio variation. The mode clusters of the selected eigenmodes (table 1) are displayed in figure 7.

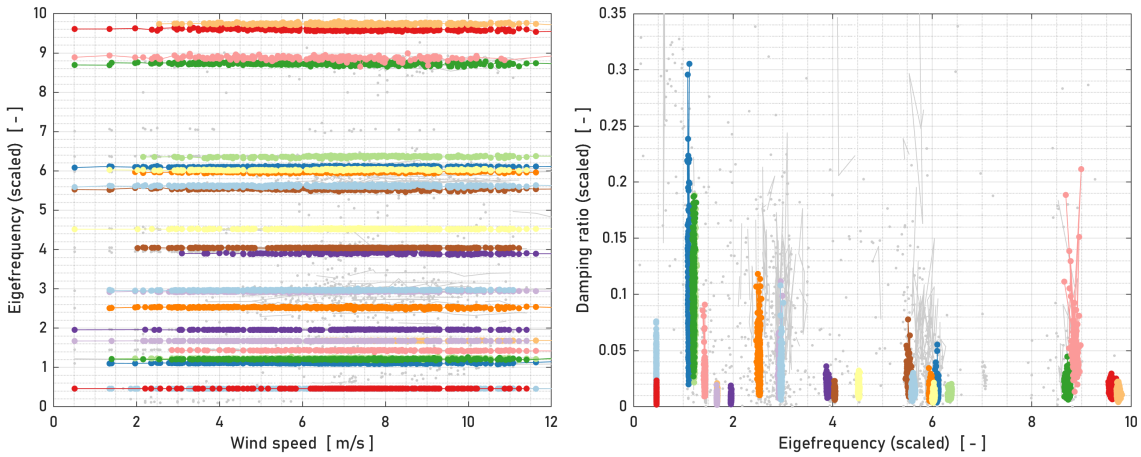


Figure 6. Tracking diagrams. Left: eigenfrequency vs wind speed. Right: eigenmode clusters. The colored markers are clusters of likely physical eigenmodes. A line connects each cluster member according to ascending wind speed. The grey points are lone spurious eigenmodes. The grey lines are mode clusters flagged as spurious because they are either too scattered or too small. See text for more details.

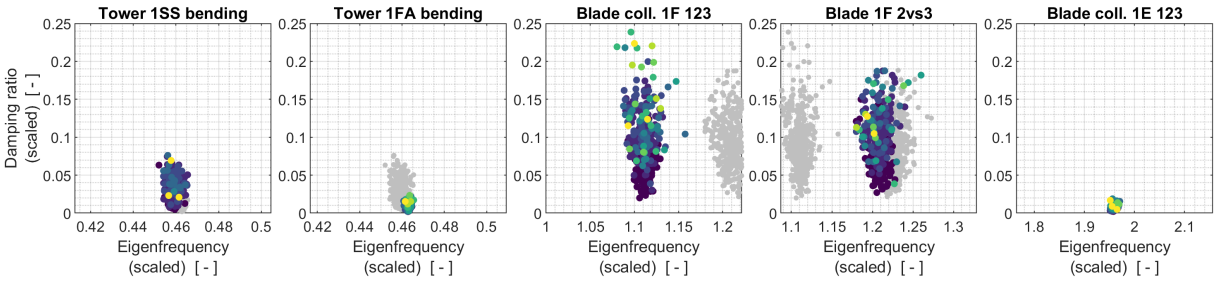


Figure 7. Damping ratio vs eigenfrequency of selected mode clusters. Neighbouring clusters are grayed-out. The color denotes the eigenfrequency variance (blue: low, yellow: high).

Mode name	median(f_n) [-]	median(ζ) [$\cdot 10^2$]
First tower side-side bending ("Tower 1SS bending")	0.459	2.8
First tower fore-aft bending ("Tower 1FA bending")	0.462	0.861
Blade collective first edge-wise bending, all blades ("Blade coll 1F 123")	1.11	9.46
Blade collective first flap-wise bending, blade 2 vs blade 3 ("Blade 1F 2vs3")	1.21	9.35
Blade collective first edge-wise bending, all blades ("Blade coll 1F 123")	1.96	0.717

Table 1. Selected modes and the median of their scaled eigenfrequency and damping ratio.

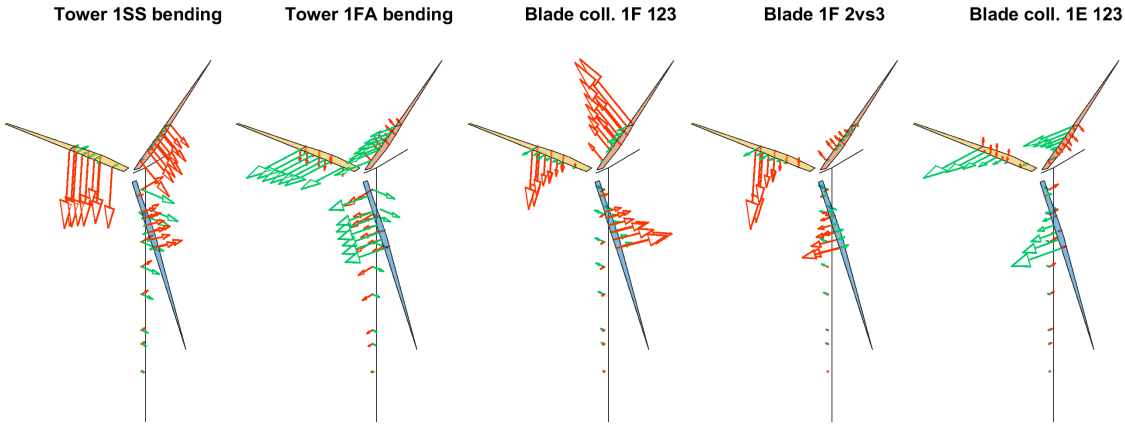


Figure 8. Selected identified mode shapes from table 1. The sensor setup is shown in figure 1.

Figure 9 shows the eigenfrequency and damping ratio variation over wind speed for the selected eigenmodes. The mode shapes that are predominant in the flap-wise (side-side) direction have higher damping than the corresponding mode shapes that act in the edge-wise (fore-aft) direction (cfr. the first tower side-side vs fore-aft bending and the first blade flap-wise and edge-wise collectives). This increase is due to aerodynamic damping increasing with wind speed. The eigenfrequency is less affected. Figure 10 displays the damping ratio as a function of the wind direction in the nacelle's reference frame. The highest damping instances are observed when the wind misalignment is low for the flap-wise (side-side) modes. The edge-wise (fore-aft) modes are less affected. Yaw misalignment increases the effective angle of attack and therefore reduces aerodynamic damping. This explains partly the damping ratio scatter observed in the previous figure. The effect of the rotor position on eigenfrequency cannot be determined conclusively because the measured wind speeds are not equally distributed among the rotor azimuth modulo 120 deg values (see figure 3). More measurements are necessary to increase confidence in the results.

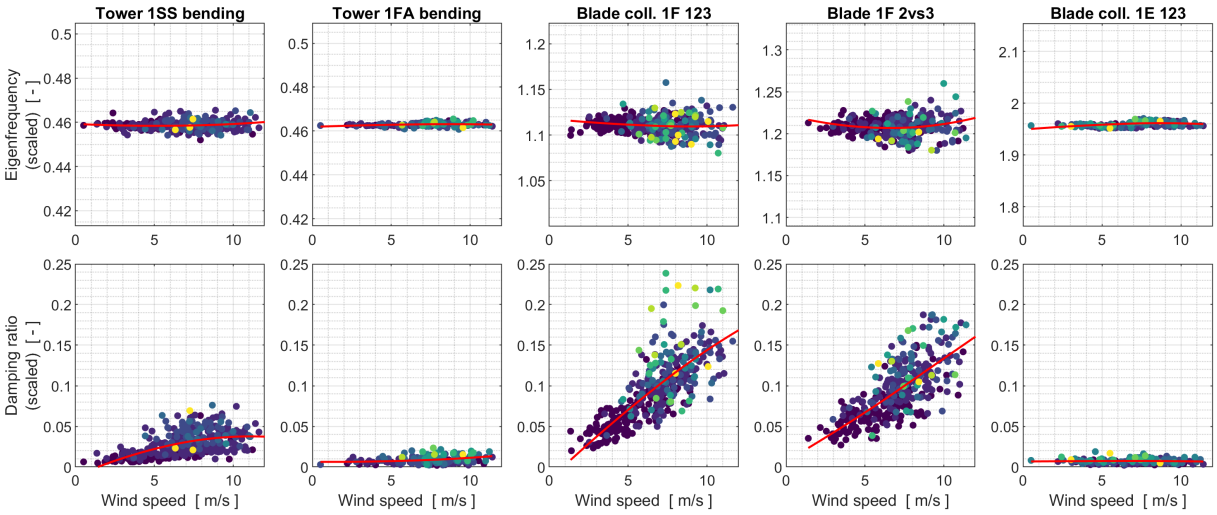


Figure 9. Eigenfrequency and damping ratio as function of wind speed. The damping axis is the same for all subplots. The damping ratio is always greater than zero. The marker color represents the pole variance (blue: low, yellow: high). The red line is a local polynomial regression of order two with a Gaussian kernel and pole variance as weighting. The mode shapes are displayed in figure 8.

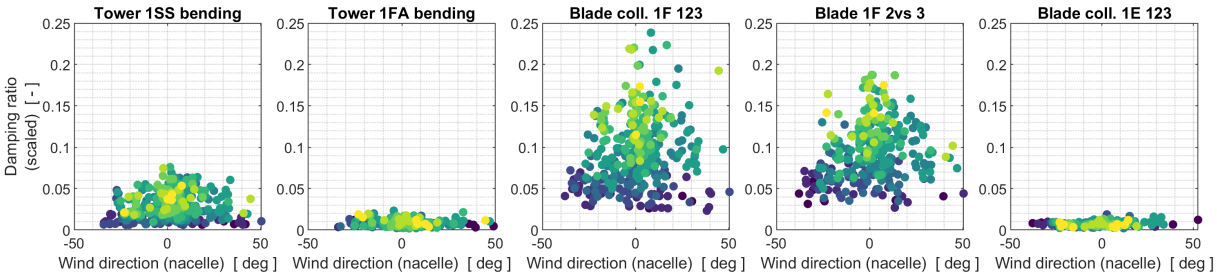


Figure 10. Damping ratio vs relative wind direction. The marker color represents the wind speed (blue: low, yellow: high). The maximal damping is achieved without yaw misalignment. Damping is always greater than zero. The eigenfrequency is less affected and not depicted here.

The modal model is assembled by selecting the "best" member of each mode cluster based on data features. The chosen data features (i.e. objective functions) are evaluated by determining their Pareto front. Next, a qDEIM model reduction algorithm [19] is applied to rank the features based on their impact. The cluster member on the Pareto front that minimizes the most impactful feature is selected for the modal model. Notice that in this approach we are mainly interested in the best eigenfrequency and mode shape estimates in order to compare them with FEM results. The chosen data features are the eigenfrequency coefficient of variation, the mode indicator function according to [20] and the mode complexity index according to [21]. Figure 11 on the left displays the cluster of the first side-side tower bending mode and the eigenmodes on its Pareto front. The auto-MAC matrix of the resulting modal model is displayed in figure 11 on the right. When assembling the modal model the tower mode shape components are projected in the nacelle's reference system (fore-aft/side-side frame). A Coleman transformation may be applied to the rotor so that all mode sets have the same rotor azimuth.

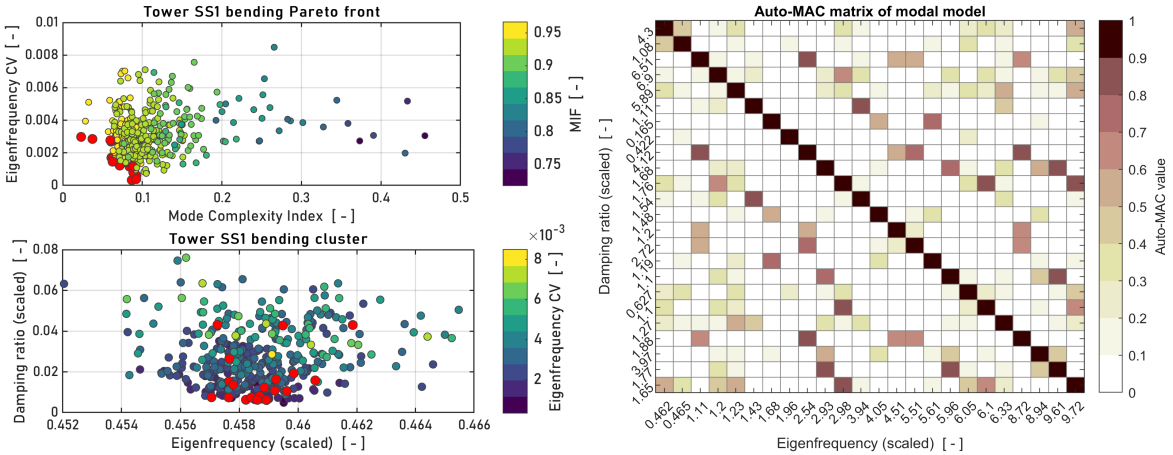


Figure 11. Modal model assembly. Left, upper subfigure: Pareto front (red dots) based on three data features of a mode cluster. Left, lower subfigure: corresponding members of one mode cluster. Right subfigure: auto-MAC matrix of resulting modal model. See text for more details.

6. Conclusions

The modal parameters of the WiValdi OPUS-2 wind turbine with locked rotor have been identified from data collected over a period of one year. Accelerometer data is acquired simultaneously from the rotor and the tower. This setup allows a better separation between rotor and tower eigenmodes. Modal analysis is performed using stochastic subspace identification. The physical poles can be estimated with low eigenfrequency variance (higher confidence). More than twenty eigenmodes can be identified and tracked for varying wind and operational conditions.

Acknowledgements

This work is part of the SysDamp Project, funded by the German Federal Ministry for Economic Affairs and Energy (*Bundesministerium für Wirtschaft und Energie*) under the contract number (*Förderkennzeichen*) 03EE3098A.

Supported by:
Federal Ministry for Economic Affairs and Energy
on the basis of a decision by the German Bundestag

References

[1] DLR 2026 Krummendeich Research Wind Farm WiValdi URL `https://windenergy-researchfarm.com/`

[2] Avendaño-Valencia L D, Chatzi E N and Tcherniak D 2020 Gaussian process models for mitigation of operational variability in the structural health monitoring of wind turbines *Mechanical Systems and Signal Processing* **142** ISSN 0888-3270 URL `https://www.sciencedirect.com/science/article/pii/S0888327020300728`

[3] Devriendt C, Magalhães F, Weijtjens W, Sitter G D, Cunha Á and Guillaume P 2014 Structural health monitoring of offshore wind turbines using automated operational modal analysis *Structural Health Monitoring* **13** 644–659 URL `https://doi.org/10.1177/1475921714556568`

[4] Jonscher C, Möller S, Liesecke L, Schuster D, Hofmeister B, Grießmann T and Rolfes R 2024 Identification Uncertainties of Bending Modes of an Onshore Wind Turbine for Vibration-Based Monitoring *Structural Control and Health Monitoring* **2024** 3280697 ISSN 1545-2255, 1545-2263 URL `https://onlinelibrary.wiley.com/doi/10.1155/2024/3280697`

[5] Hermes A, Greś S and Riva R 2025 Uncertainty propagation and subspace identification of isotropic wind turbines with the PO-MOESP algorithm *Mechanical Systems and Signal Processing* **238** 113159 ISSN 08883270 URL `https://linkinghub.elsevier.com/retrieve/pii/S088832702500860X`

[6] Gnebner K and Govers Y 2024 Operational modal analysis of the idling cart3 research wind turbine using bladevision data *10th International Operational Modal Analysis Conference, IOMAC 2024* (*Lecture Notes in Civil Engineering* vol 515) (Springer, Cham) pp 638–648 ISBN 978-303161420-0 URL `https://elib.dlr.de/206902/`

[7] Gnebner K, Govers Y, Sinske J, Buchbach R, Kober P and Jelicic G 2025 Identification and long-term tracking of modal parameters of a 150m wind measurement mast using ambient excitation *11th International Operational Modal Analysis Conference, IOMAC 2025* International Operational Modal Analysis Conference (IOMAC 2025) ed Döhler M, Mélot A and López M A (INTERNATIONAL GROUP OF OPERATIONAL MODAL ANALYSIS) pp 434–444 ISBN 978-840975120-4 URL `https://elib.dlr.de/216574/`

[8] Govers Y, Gnebner K and Jelicic G 2025 Reliable damping ratio estimates from a 50m+ wind turbine rotor blade as a guide for prototype testing in the low frequency regime *11th International Operational Modal Analysis Conference, IOMAC 2025* ed Döhler M, Mélot A and Manuel Aenlle L ISBN 978-840975120-4 URL `https://elib.dlr.de/221467/`

[9] Gnebner K and Govers Y 2024 Operational modal analysis of the idling CART3 research wind turbine using bladevision data *10th International Operational Modal Analysis Conference, IOMAC 2024* (*Lecture Notes in Civil Engineering* vol 515) (Springer, Cham) pp 638–648

[10] Reynders E, Pintelon R and Roeck G D 2008 Uncertainty bounds on modal parameters obtained from stochastic subspace identification *Mechanical Systems and Signal Processing* **22** 948–969 ISSN 0888-3270

[11] Verhaegen M 2013 Subspace Techniques in System Identification *Encyclopedia of Systems and Control* ed Baillieul J and Samad T (London: Springer London) pp 1–13 ISBN 978-1-4471-5102-9 URL https://doi.org/10.1007/978-1-4471-5102-9$_1$07 − 1

[12] Bir G 2008 Multi-Blade Coordinate Transformation and its Application to Wind Turbine Analysis *46th AIAA Aerospace Sciences Meeting and Exhibit* (Reno, Nevada: American Institute of Aeronautics and Astronautics) ISBN 978-1-62410-128-1 URL https://arc.aiaa.org/doi/10.2514/6.2008-1300

[13] Jelicic G 2022 *System Identification of Parameter-Varying Aeroelastic Systems using Real-Time Operational Modal Analysis* Ph.D. thesis Syddansk Universitet (SDU) URL https://elib.dlr.de/187222/

[14] Epps B P and Krivitzky E M 2019 Singular value decomposition of noisy data: mode corruption *Experiments in Fluids* **60** 121 ISSN 0723-4864, 1432-1114 URL http://link.springer.com/10.1007/s00348-019-2761-y

[15] Reynders E, Houbrechts J and Roeck G D 2012 Fully automated (operational) modal analysis *Mechanical Systems and Signal Processing* **29** 228–250 ISSN 0888-3270 URL https://www.sciencedirect.com/science/article/pii/S0888327012000088

[16] Goursat M, Döhler M, Mevel L and Andersen P 2011 Crystal Clear SSI for Operational Modal Analysis of Aerospace Vehicles *Conference Proceedings of the Society for Experimental Mechanics Series* (*Structural Dynamics* vol 3) (Springer) pp 1421–1430 ISBN 978-1-4419-9833-0

[17] Luspay T, Péni T, Gőzse I, Szabó Z and Vanek B 2018 Model reduction for LPV systems based on approximate modal decomposition *International Journal for Numerical Methods in Engineering* **113** 891–909

[18] Vacher P, Jacquier B and Bucharles A 2010 Extensions of the MAC criterion to complex modes *International Conference on Noise and Vibration Engineering 2010 (ISMA 2010)* (Leuven: Katholieke Universiteit Leuven, Department of Mechanical Engineering) ISBN 978-1-61782-277-3

[19] Drmač Z and Gugercin S 2016 A new selection operator for the discrete empirical interpolation method—improved a priori error bound and extensions *SIAM Journal on Scientific Computing* **38** A631–A648 URL https://doi.org/10.1137/15M1019271

[20] Breitbach E J 1988 Recent developments in multiple input modal analysis *Journal of Vibration, Acoustics, Stress, and Reliability in Design* **110** 478–484 ISSN 0739-3717 URL https://doi.org/10.1115/1.3269554

[21] Cabboi A, Magalhães F, Gentile C and Cunha Á 2017 Automated modal identification and tracking: Application to an iron arch bridge *Structural Control and Health Monitoring* **24** e1854 _eprint: https://onlinelibrary.wiley.com/doi/pdf/10.1002/stc.1854 URL https://onlinelibrary.wiley.com/doi/abs/10.1002/stc.1854